ARTICLE

First-Principles Study of La Doping Effects on the Electronic Structures and Photocatalytic Properties of Anatase TiO_2

Ping Huang, Bo Shang*, Ling-jie Li, Jing-lei Lei

School of Chemistry and Chemical Engineering, Chongqing University, Chongqing 400044, China

(Dated: Received on March 12, 2015; Accepted on June 16, 2015)

The effects of doping concentration, position and oxygen vacancy defect on the stability, electronic and optical properties of La-doped anatase TiO_2 have been investigated based on DFT+U method. The calculations indicated that the doping concentration and sites of La affected the stability and band gap of La-doped TiO_2 significantly due to the lattice distortion, which obey the ionic Pauling's rules and crystal field theories; moreover, the simulated adsorption spectrum shows an obviously increase in the photocatalysis properties, which are in good agreement with recently experimental measurements. The oxygen vacancy defect will enhance the structural stability and the adsorption of visible light in La-doped TiO_2 system, which is important in photocatalytic application.

Key words: Density functional theory, La doping, Anatase TiO_2, Oxygen vacancy

I. INTRODUCTION

Titanium dioxide (TiO_2) has been found to be a promising material for photocatalytic degradation of harmful organic compounds due to its excellent properties such as biological and chemical inertness, stability to corrosion, non-toxicity, and relatively low cost [1, 2]. However, the use of TiO_2 is impaired by its wide band gap (3.2 eV for anatase), which requires ultraviolet irradiation for photocatalysis. For increased utility of TiO_2, it is highly recommended to shift its absorption edge towards visible light, which constitutes the major part (about 50%) of solar energy [3]. Among the various methods, doping of foreign atoms in the TiO_2 lattice is found to be a promising approach to shift its absorption edge towards visible light and improve the photocatalytic activity of TiO_2 [4, 5].

Metal and nonmetal doping in TiO_2 has been widely studied for improving its visible-light photocatalytic activity [6, 7]. Nitrogen (N) doping in TiO_2 has been widely studied via experimental [8, 9] and theoretical [10−13] techniques, and found to be a successful method for extending the absorption edge of TiO_2 towards the visible region. Dai *et al.* found that the dopant location and the dopant concentration will affect the band structure of the defective TiO_2 system and play a major role in obtaining better electronic and optical properties [12, 13]. Among the metals, the rare earth ions can offer the advantage of transitions in the visible region, many studies have focused on the luminescence properties of rare earth elements hosted in crystalline matrices [14, 15], especially in TiO_2 [16−27]. Jing *et al.* synthesized the La doped TiO_2 nanoparticles by sol-gel method with the concentrations ranging from 0.5mol% to 3mol% and found that the La-TiO_2 with 1mol% (873 K) molar ratio gave the best activity [19]. Similar results were also found by Zhang *et al.* while investigation of the photoelectric conversion efficiency in the dye-sensitized solar cells was fabricated from La-doped TiO_2 [20].

In theory, much work has been reported recently in this field [28−33]. Zhao *et al.* investigated the lanthanide doping TiO_2 with density functional theory (DFT) and indicated that lanthanide doping could remarkably improve the photocatalytic activity of TiO_2 [28]. Gao *et al.* showed that La and Y doping could enhance the redox potential of TiO_2 dramatically and shift the absorption edges of doped TiO_2 toward the ultraviolet region [29]. However, the effects of doping concentration, position and O vacancy have not been investigated, which will help to understand the mechanism of band gap narrowing.

In this work, the first principles calculations were performed to get the geometrical, electronic, and optical properties of La-doped anatase TiO_2 by considering the effect of doping concentration, sites and O vacancy. It is hoped that this study will provide the theoretical rationale and guidance to the design and construction of new effective photocatalyst in the practical future.

II. COMPUTATIONAL DETAILS

All the calculations were performed with the Vienna *ab initio* simulation package (VASP) [34, 35]. Both the generalized gradient approximation (GGA) and DFT+U methods have been employed, and in both cases the PAW-PBE method was adopted to describe

*Author to whom correspondence should be addressed. E-mail: bshang@cqu.edu.cn, Tel.: +86-13983858642

the interaction between electrons and ions [36−39]. For higher accuracy, the O ($2s^2 2p^4$), Ti ($3s^2 3p^6 3d^2 4s^2$) and La ($5s^2 5p^6 5d^1 6s^2$) electrons were considered as valence states, and a kinetic cutoff energy of 450 eV was chosen. For the crystal calculation, the Monkhorst-Park scheme [40] k-point grids sampling was set at 5×5×3 in the supercell. The structures were relaxed using a conjugate gradient minimization algorithm until the magnitude of residual Hellman-Feynman force on each atom was less than 0.05 eV/Å [41].

The DFT+U method has been employed in order to accurately describe the electronic structure and the strong on-site Coulomb repulsion among the localized transition/rare earth metal d/f electrons. The choice of U is, however, ambiguous and it is not trivial to determine the value, though there are attempts to extract it from standard First-principles calculations. Hence, U is often fitted to reproduce a certain set of experimental data, such as band gaps and structural properties. We used the approach formulated by Dudarev *et al.* [42]. The function is shown in the following

$$E_{\mathrm{DFT}+U} = E_{\mathrm{DFT}} + (U-J)\sum_{\sigma}\frac{\mathrm{Tr}(\rho^{\sigma}-\rho^{\sigma}\rho^{\sigma})}{2} \quad (1)$$

where ρ^{σ} denotes the spin σ polarized on-site density matrix. The spherically averaged Hubbard parameter U describes the increase in energy caused by placing an extra electron at a particular site, and the parameter J (1 eV) represents the screened exchange energy. The effective Hubbard parameter, U_{eff}=U−J, which accounts for the on-site Coulomb repulsion for each affected orbital, is the only external parameter required in this approach. In this work, the U of 8.2 eV for Ti3d was selected from previous work about metal oxides [43−46]. Suitable Hubbard U parameters used in the calculations were determined by the band gap of the system. We found that the band gap of the system with U=8.2 eV added to Ti agrees with the previous calculation [47] and the experimental results [49] much better. Moreover, the lattice parameters of pure anatase TiO_2 were optimized to be a=b=3.776 Å and c=9.486 Å, which are in good agreement with the experimental values (a=b=3.785 Å, c=9.512 Å) [50], as well as theoretical results with PBE, a=b=3.800 Å, c=9.670 Å [51]. This implies that the DFT+U approach with adopted parameters in our calculations may produce reasonable results.

The spectra were simulated based on the electric dipole approximation. From the view point of quantum mechanics, the interaction of a photon with the electrons in the system is described in terms of time dependent perturbations of the electronic ground states. The straight forward transition rates between occupied and unoccupied states, which are caused by photon absorption are determined by the electronic structures. Therefore, according to Fermi's golden rule, the imaginary part of the dielectric function ε_2 can be calculated as the following formula:

$$\varepsilon_2(q\to \mathrm{O}_{\mu}, h\omega) = \frac{2e^2\pi}{\Omega\varepsilon_0}\sum_{K,\mathrm{V},\mathrm{C}}\left|\left\langle\psi_K^{\mathrm{C}}\left|\mu\cdot\gamma\right|\psi_K^{\mathrm{V}}\right\rangle\right|^2\cdot \delta\left(E_K^{\mathrm{C}}-E_K^{\mathrm{V}}-E\right) \quad (2)$$

where μ is the vector defining the polarization of the incident electric field, C and V represent the conduction band (CB) and the valence band (VB), respectively, K represents the reciprocal lattice vector, $\left|\left\langle\psi_K^{\mathrm{C}}\left|\mu\cdot\gamma\right|\psi_K^{\mathrm{V}}\right\rangle\right|^2$ is the matrix of momentum transition, E_K^{C} and E_K^{V} represents the intrinsic level in CB and VB. Since the dielectric function describes a causal response, its real part ε_1 and imaginary part ε_2 are connected with a Kramers-Kronig transform, and ε_2 is related to the absorption coefficient α by

$$\alpha(\omega) = \frac{2\omega}{c}\left\{\left[\varepsilon_1^2(\omega)+\varepsilon_2^2(\omega)\right]^{1/2}-\varepsilon_1(\omega)\right\}^{1/2} \quad (3)$$

where c is light velocity in vacuum.

The structures of La-doped anatase TiO_2 are modeled by replacing Ti with La in a 48 atoms 2×2×1 supercell. The species that n Ti atoms are replaced by n La atoms are named as n-TiO_2 (Fig.1(a)). For the different substituting position of La, all models are built based on the 2-TiO_2 system, named as (1,2)-, (1,3)-, (1,7)-, and (3,5)-TiO_2.

III. RESULTS AND DISCUSSION

A. Different concentrations of La-doped TiO_2

We initiated the investigation with the concentration effect. All the six types of models are based on the pure 48 atoms 2×2×1 anatase supercell; where 16−n (n=1−6) Ti atoms are replaced with La, as shown in Fig.1(a). The corresponding atomic concentrations of impurity are 2.08%, 4.17%, 6.25%, 8.33%, 10.42%, and 12.5% (atom fraction) in total. In addition, the doping sites effect is not taken into account, which will be discussed in later section.

To examine the efficiency of doping level, we define the relative binding energy ΔE_{b} compared with pure anatase TiO_2 according to the following equation [30]:

$$\Delta E_{\mathrm{b}} = \frac{1}{n}(E_{\mathrm{doped}} - E_{\mathrm{pure}} + \Delta n_{\mathrm{Ti}}\mu_{\mathrm{Ti}} - \Delta n_{\mathrm{La}}\mu_{\mathrm{La}}) \quad (4)$$

where E_{doped} and E_{pure} are the total energy of doped-TiO_2 and pure TiO_2 in the same supercell, μ_{Ti} and μ_{La} represent the chemical potential of La and Ti atom, which is generated from the bulk metal, respectively. n refers to the number of atoms per supercell and Δn is the change atoms due to the doping (n_{Ti}=n_{La}). According to the results, which are listed in Table I, ΔE_{b} for all doped-TiO_2 systems are above zero (the lowest one is 3.74 eV for 1-TiO_2 system), which means

DOI:10.1063/1674-0068/28/cjcp1503038

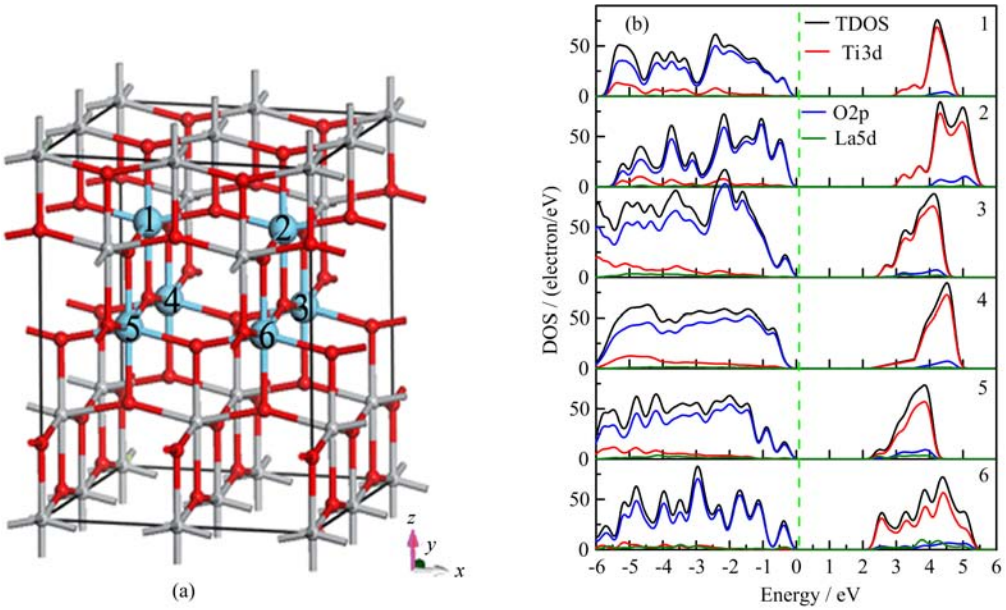

FIG. 1 (a) Calculated model of different La doping level systems. Gray spheres and red spheres represent the Ti and O atoms, respectively. The blue spheres are the La atom, where the digitals mean the name of La atoms which will be replaced. The species that n Ti atoms are replaced by n La atoms are named as n-TiO_2 (n=1−6). (b) Total/projected density of states (TDOS/PDOS). Black line denotes the total DOS, red line denotes the Ti3d states, blue line denotes the O2p states, and green line denotes the La5d states.

TABLE I The relative binding energy ΔE_b, band gap, lattice parameters, and average bond-length in three axial directions at different La doping level.

Species	ΔE_b/eV	Band gap/eV	Lattice parameter/Å			ΔV/%	Ti−O bond length/Å		
			a	b	c		x axis	y axis	z axis
Pure-TiO_2	–	3.11	3.776	3.776	9.486	–	1.93	1.93	1.98
1-TiO_2	3.74	2.84	3.798	3.798	10.099	7.7	1.92	1.92	2.0
2-TiO_2	3.81	2.78	3.839	3.763	10.570	12.9	1.92	1.87	1.99
3-TiO_2	3.87	2.65	3.889	3.914	10.015	12.7	1.98	1.97	1.98
4-TiO_2	3.80	2.39	3.859	3.859	10.745	18.3	1.88	1.88	2.11
5-TiO_2	3.89	2.11	3.874	3.876	11.542	28.1	1.97	1.92	1.94
6-TiO_2	3.84	2.09	3.936	3.917	11.732	33.7	1.95	1.94	1.89

that stability will decrease after La doping. For the 3-TiO_2 and 5-TiO_2, ΔE_b are 3.81 and 3.89 eV, which are greater than that of the neighborhood. This odd-even phenomenon might be caused by doping symmetry and doping sites, which will be discussed in the next part.

The band gap is described as in Table I. With the increase of the doping level, the band gap decreased dramatically, from 3.11 eV for pure TiO_2 to 2.09 eV for 6-TiO_2. The band gap narrowing will cause an enhancement of visible-light absorption and photocatalytic performance, which agree quite well with experimental results [21−23]. The lattice volume of pure TiO_2 is 135.25 $Å^3$ and the band gap is 3.11 eV. For the 1-TiO_2, lattice volume increases by 7.7% compared with pure TiO_2, and the band gap drops to 2.84 eV. For the 2-TiO_2 and 6-TiO_2, lattice volume increases by 12.9% and 33.7%, while the band gap is 2.78 and 2.09 eV, respectively. As the ionic radius of La^{3+} (1.04 Å) is much larger than that of Ti^{4+} (0.61 Å) [24, 25], after high level doping, the lattice volume increased significantly, which will cause phase transformation and will not be considered in this work. However, with a lower doping level, the band gap will decrease and the stability can also be guaranteed. Hence, a proper doping level will be selected in the application.

In order to explore the band gap narrowing mechanism, we present the projected density of states (PDOS) for all atoms in Fig.1(b). In order to compare the DOS/PDOS of different systems directly, we have made some adjustment on the DOS/PDOS figure. All the DOS/PDOS figures in this work, the 0 position refers to the valence band maximum but not Fermi level. The PDOS show that the most contribution of the valence

DOI:10.1063/1674-0068/28/cjcp1503038

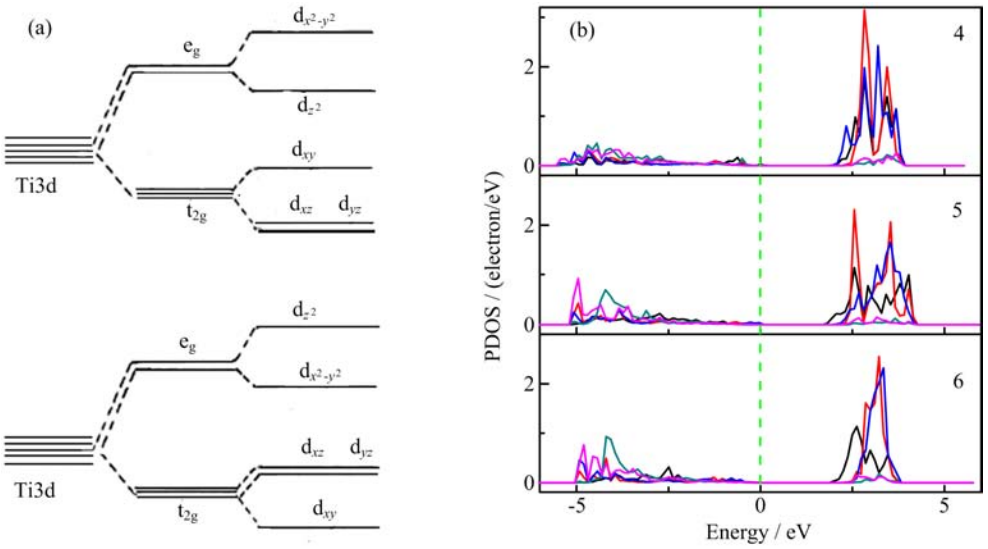

FIG. 2 (a) Schematic representations of energy levels splitting by distortion to anatase TiO_2 with octahedron elongated along the z-axis and squashed octahedron along the z-axis, (b) PDOS of Ti3d states for different concentration systems. Black, red, blue, green, and pink lines denote Ti d_{xy}, d_{xz}, d_{yz}, and $d_{x^2-y^2}$, respectively.

band edge (VBE) is O2p states and the conduction band edge (CBE) is Ti3d states, which are the same as those obtained from pure bulk TiO_2 [31]. PDOS further confirm that the La doping states are delocalized and the band gap narrowing is caused by the move down of unoccupied Ti3d orbital. Interestingly, the bottom of the conduction band is occupied by Ti3d states for all doped systems.

The relationship between the movement of the Ti unoccupied 3d states and the distortion can be interpreted with the crystal field theory (CFT) [52]. The Ti−O bond lengthes of doped systems are also listed in Table I. The Ti−O in pure TiO_2 is 1.93 Å in x and y axis and 1.98 Å to z axis, which are in good agreement with the present results [32]. The Ti−O bond length in all doped systems is changed compared to that of pure TiO_2. Two kinds of change can be found, *e.g.*, in the 4-TiO_2, the bond length in the z axis is stretched to 2.11 Å but shortened to 1.88 Å in x and y axis, which give rise to an elongated octahedral pyramid, while in 6-TiO_2 system, the average bond length is shortened to 1.89 Å in z axis but elongated to 1.99 and 1.94 Å in x and y axis, which brought about a squashed octahedral pyramid. As a six-coordinated octahedral structure, the d orbital energy splitting is set out in Fig.2(a). Without distortion, d orbital spitted into two degeneracy groups, with the symmetry, $e_g(d_{x^2-y^2},d_{z^2})$ and $t_{2g}(d_{xz},d_{yz},d_{xy})$. In the elongated octahedron along the z-axis, the energy of $d_{x^2-y^2}$ orbital is higher than the d_{z^2} orbital and the energies of d_{xz} and d_{yz} orbital are lower than that of d_{xy}. Otherwise, in squashed octahedron along the z-axis, the d_{xz}, d_{yz}, and d_{z^2} energies increase and the others decrease. The CFT inference is confirmed by our PDOS results, as shown in Fig.2(b). For elongated 4-TiO_2 model, the bottom of the conduction band is mainly composed of Ti3d_{xz} state while in the 5-TiO_2 and 6-TiO_2 they are the Ti3d_{xy} state.

It is shown that the narrowing of band gap mainly contributes to the splitting of Ti3d orbital which roots in the structural distortion. The structural distortion is increased with the doping level. However, the relationship between the stability and band gap with the doping level is not an ordinary linear relationship, as the doping level increases, the structure distorts significantly, which will lead to a narrowing of the band gap but a decreasing of the stability, illustrating that the distortions also depend on the doping sites; that is why further investigation of different La doping sites will be extremely necessary.

B. Different La substituting sites

The simplest two atoms doping system has been studied. There are four possible nonequivalent sties in 2×2×1 supercell with the doping concentration of 4%, namely (1,2)-, (1,3)-, (1,7)-, and (3,5)-TiO_2. The La octahedrons have been drawn as shown in Fig.3(a). For the (1,7)-TiO_2, the cell parameter has been changed from (a=b=3.776 Å, c=9.486 Å) to (a=b=3.932 Å, c=10.266 Å) after full optimization, which means the doping will increase the volume of the cell by 15%. This result coincides with that of the current date in the experiment [26].

The stability of systems with different doping sites can be judged by ΔE_b, as shown in Table II. For the (1,7)-TiO_2 and (1,3)-TiO_2, ΔE_b is very similar and a little lower than the other two systems. It states that stabilities are closely bound up to the distances of the most neighboring doping atoms. For the (1,7)-TiO_2,

DOI:10.1063/1674-0068/28/cjcp1503038

TABLE II The relative binding energy ΔE_b, band gap, lattice parameters, and average bond length of the supercell in axial directions at different doping sites.

Name	ΔE_b/eV	Band gap/eV	Lattice parameter/Å			Ti−O bond length/Å		
			a	b	c	x axis	y axis	z axis
Pure-TiO_2	–	3.11	3.776	3.776	9.486	1.93	1.93	1.98
(1,2)-TiO_2	3.81	2.78	3.839	3.763	10.570	1.92	1.87	1.99
(1,3)-TiO_2	3.74	2.79	3.552	3.825	10.377	1.94	1.91	1.96
(1,7)-TiO_2	3.71	2.81	3.932	3.932	10.266	1.96	1.91	2.01
(3,5)-TiO_2	3.79	2.71	3.378	3.689	10.566	1.88	1.88	2.03

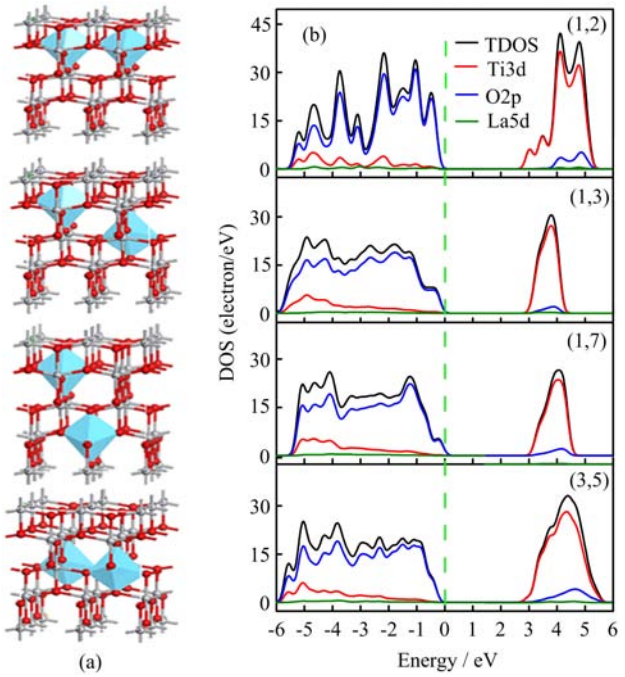

FIG. 3 (a) Calculated model of different La substitute position systems. Gray spheres and red spheres are the Ti and O atoms, respectively. The blue octahedrons are the La atoms. (b) Total/projected density of states (TDOS/PDOS). Black line denotes the total DOS, red line denotes the Ti3d state, blue line denotes the O2p state, and green line denotes the La5d states.

the nearest distance of two La atoms is 5.443 Å. While in the (1,2)-TiO_2, the distance is 3.776 Å, as a result, the (1,7)-TiO_2 has a lower relative binding energy. The stability of these different doping sites can be interpreted with the ionic Pauling's Rules [53]. For anatase TiO_2, structure is based on octahedrons which share four O−O edges, while doped with La, some of the Ti octahedrons are replaced by La octahedron. Based on the Pauling's Rules of three and four, in a crystal containing different cations, those of high value and small coordination number don't often share polyhedron elements with one another. Different kinds of doping types will slightly change the polyhedron elements sharing. In the (1,2)-TiO_2, the La octahedron share the vertex, and thus with a higher energy. For the other three systems, the sharing of O−O edge between octahedrons of TiO_2 will decrease, which will enhance the stability.

To find the effects of doping position on the electronic properties of La-doped TiO_2, the total DOS and PDOS have been established (Fig.3(b)). The calculated band gaps of TiO_2 with distinct sites of La doping are 2.78, 2.79, 2.81, and 2.71 eV, respectively. Band gap differences between separate doping sites are not significant in comparasion with that of different doping concentration. The conduction bands are wildly extended in the PDOS of (1,2)-TiO_2 and (3,5)-TiO_2 while localized at a higher peak in the (1,3)-TiO_2 and (1,7)-TiO_2. The results of the band gap and the lattice distortion coincide, as shown in Table II. In the (1,3)-TiO_2, the bond length of Ti−O is slightly changed from pure anatase and its band gap is 2.79 eV, and in the (3,5)-TiO_2, bond length of Ti−O change much bigger, which results in the band gap of 2.71 eV.

From the simulated spectra in Fig.4, it is noted that the absorption spectrum is cut off at ∼440 nm, the band gap is narrowed to 2.81 eV and the absorbance intensity in the wavelength range from 380 nm to 440 nm is increased obviously. Such light absorbance enhancement in the visible light range corresponds roughly to values obtained in the experiment [33].

From the doping sites effect on the stability and electronic properties, it is found that the stabilities of the system are mainly affected by the distance of two neighboring doping atoms in the supercell, which obeys the ionic Pauling's Rules. Doping sites prefer to spread separately to gain higher stability, which will result in less band gap narrowing. However, sites reduced band gap narrowing is not as significant as the concentration effect. Finally, we found that in the (1,7)-TiO_2 type material, the 4% is the just doping level, which can decrease the band gap from UV to blue light and still obey the ionic Pauling's rules. The calculated band gap of this system is 2.81 eV and absorption shifts from UV-light region to visible-light region, which makes it applicable to practice.

C. Oxygen vacancy defect

In the study of La-doped TiO_2 system, charge compensation needs to be considered while Ti^{4+} is sub-

DOI:10.1063/1674-0068/28/cjcp1503038

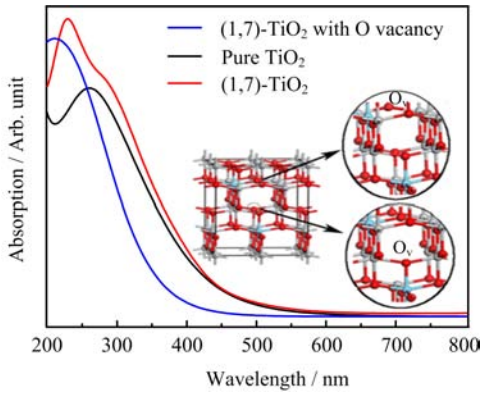

FIG. 4 Optical absorption curves of pure TiO_2, (1,7)-TiO_2, and (1,7)-TiO_2 with O vacancy. The black line denotes the pure TiO_2, red line denotes (1,7)-TiO_2, and blue line denotes (1,7)-TiO_2 with O vacancy.

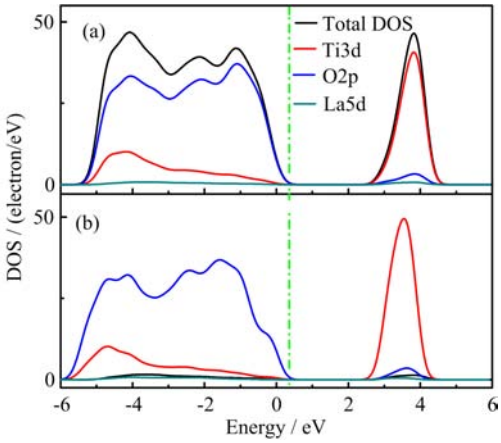

FIG. 5 DOS of (1,7)-TiO_2 system (a) with an oxygen vacancy defect and (b) without oxygen vacancy defect. Black line denotes the total DOS, red line denotes the Ti3d state, blue line denotes the O2p state, and green line denotes the La5d state.

stituted by impurities with La^{3+}. To meet the electronic neutrality of the entire system, oxygen vacancies are inevitable when a high-valence host ion is substituted by a low-valence guest ion. In order to investigate the effect of oxygen vacancy on electronic structures of La-TiO_2, we calculated the electronic structures of La doped TiO_2 with oxygen vacancy defect. We investigated two La dopants incorporated into the TiO_2 and the formation of an oxygen vacancy since this system retains electronic neutrality. In the previous section, we found that the (1, 7)-TiO_2 was the most stable models with two La atoms doping.

For the (1,7)-TiO_2 with O vacancies, ΔE_b is 3.67 eV, which is 0.04 eV lower than that of (1,7)-TiO_2, explaining that O vacancies will enhance stability of La doping TiO_2. Two types of models with O vacancies have been considered, as shown in Fig.4. The DOS of two La atoms doped TiO_2 with and without oxygen vacancy defect is shown in Fig.5. Figure 5(b) shows a tiny change of the band gap in comparison with the DOS of La-doped TiO_2 without O vacancy. The top of the valence band is occupied by O vacancy states, and the band gap of (1,7)-TiO_2 with O vacancy is 2.87 eV which is slightly larger than that without O vacancy system (2.81 eV). Doping with two La atoms in combination with an O vacancy does not introduce any defect level in the band gap, since the excess electrons induced by the La are compensated by the O vacancy. The Ti3d level is located above the valance band that is expected to hybridize with oxygen defect states and then enhance the adsorption of the UV light. In all, the results indicated that oxygen vacancy defect could not only make the structure of (1,7)-TiO_2 more stable but also enhance the adsorption of UV light while in La-doped TiO_2 system, this result is in agreement with the report in Ref.[27].

It also clearly shows that the absorbance enhanced in UV region after the introduced of O vacancy (Fig.4). The photocatalysis is totally affected by the band gap, electron-hole recovery rate, and the photon adsorption effect. From the electronic and optical calculations, we found that La doping will enhance the photocatalysis effect via band gap engineering and the improvement of adsorption efficiency, which illustrate the agreement with experiment. The presence of O vacancy in La doped TiO_2 will slow down the recombination rate of electron-hole pairs due to the cooperation of dopants and vacancy states, which could enhance the photocatalytic efficiency of doped TiO_2.

IV. CONCLUSION

The doping concentration and position effects on the stability, electronic and optical properties of La-doped anatase TiO_2 have been investigated based on first-principles density functional theory. The calculation shows that the structural stability and the band gap of La-doped TiO_2 are mainly controlled by the concentration of La. Structural stability decreased and the band gap narrowed with the increase of La doping concentration. The band gap narrowed as a consequence of Ti3d orbit splitting root in the lattice distortion due to the doping concentration and sites. Increases in photocatalysis of La-doping TiO_2 mainly contribute to the band gap narrowing and enhancement of adsorption. The results of the electronic structures of two La atoms doping TiO_2 systems with an O vacancy indicated that the O vacancy should make the structure more stable and alter the light absorption of TiO_2 in the UV light region. The O vacancy is important in the unbiased charged doping, which could not be omitted. Finally, based on the ionic Pauling's rules, a proper density of La doping has been suggested, which has a remarkable stability and a proper band gap, and might be appropriate for photocatalysis.

DOI:10.1063/1674-0068/28/cjcp1503038

V. ACKNOWLEDGMENTS

This work was supported by the National Natural Science Foundation of China (No.21273293 and No.21373281), the Program for New Century Excellent Talents in University (No.NCET-12-0587 and No.NCET-13-0633), the National Science Foundation Project of CQ CSTC (No.020005303100), and the Fundamental Research Funds for the Central Universities.

[1] K. G. Grigorov, I. C. Oliveira, H. S. Maciel, M. Massi, J. M. S. Oliveira, J. Amorim, and C. A. Cunha, Surf. Sci. **605**, 775 (2011).
[2] Y. Ma, J. Zhang, B. Tian, F. L. Chen, and J. Wang, J. Hazard. Mater. **82**, 386 (2010).
[3] Y. Su, Y. Xiao, Y. Li, Y. Du, and Y. Zhang, Mater. Chem. Phys. **126**, 761 (2011).
[4] C. He, Y. Yu, X. Hu, and A. Larbot, Appl. Surf. Sci. **200**, 239 (2012).
[5] I. E. Saliby, L. Erdei, H. K. Shon, and J. H. Kim, J. Ind. Eng. Chem. **17**, 358 (2011).
[6] V. C. Stengl and S. Bakardjieva, J. Phys. Chem. C **114**, 19308 (2010).
[7] X. Yu, C. Li, H. Tang, Y. Ling, T. A. Tang, and Q. Wu, J. Kong, Comput. Mater. Sci. **49**, 430 (2010).
[8] F. Peng, Y. Liu, H. J. Wang, H. Yu, and J. Yang, Chin. J. Chem. Phys. **23**, 437 (2010).
[9] F. Spadavecchia, G. Cappelletti, S. Ardizzone, M. Ceotto, and L. Falciola, J. Phys. Chem. C **115**, 6381 (2011).
[10] X. Han and G. Shao, J. Phys. Chem. C **115**, 8274 (2011).
[11] L. Jia, C. Wu, S. Han, N. Yao, Y. Li, Z. Li, B. Chi, J. Pu, and L. Jian, J. Alloys Compd. **509**, 6067 (2011).
[12] K. Yang, Y. Dai, B. Huang, and S. Han, J. Phys. Chem. B **110**, 24011 (2006).
[13] K. Yang, Y. Dai, and B. Huang, J. Phys. Chem. C **111**, 12086 (2007).
[14] J. Zhu, K. Zhu, and L. Chen, J. Non-Cryst. Sol. **352**, 150 (2006).
[15] J. C. Gacon, K. Horchani, A. Jouini, C. Dujardin, and I. Kamenskikh, Opt. Mater. **28**, 14 (2006).
[16] C. Y. Huang, L. C. Zhang, and X. H. Li, Chin. J. Catal. **29**, 163 (2008).
[17] K. M. Parida and N. Sahu, J. Mol. Catal. A **287**, 151 (2008).
[18] L. J. Li, Z. Q. Zhou, J. L. Lei, J. X. He, P. P. Liu, and F. S. Pan, Mater. Lett. **79**, 252 (2012).
[19] L. Q. Jing, X. J. Sun, B. F. Xin, B. Q. Wang, W. M. Cai, and H. G. Fu, J. Sol. State Chem. **177**, 3375 (2004).
[20] J. Y. Zhang, Z. Y. Zhao, X. Y. Wang, T. Yu, J. Guan, Z. T. Yu, Z. S. Li, and Z. G. Zou, J. Phys. Chem. C **114**, 18396 (2010).
[21] C. Liang and F. Li, Dyes Pigments **76**, 477 (2008).
[22] W. Zhou, Y. H. Zheng, and G. H. Wu, Appl. Surf. Sci. **253**, 1387 (2006).
[23] Y. Q. Wang, H. M. Cheng, Y. Z. Hao, J. M. Ma, W. H. Li, and S. M. Cai, Thin Solid Films **349**, 120 (1999).
[24] Y. H. Zhang, H. X. Zhang, Y. X. Xu, and Y. G. Wang, J. Sol. State Chem. **177**, 3490 (2004).
[25] Y. H. Zhang and A. Reller, Mater. Lett. **57**, 4108 (2003).
[26] L. Q. Jing, X. J. Sun, B. F. Xin, B. Q. Wang, W. M. Cai, and H. G. Fu, J. Sol. State Chem. **177**, 3375 (2004).
[27] Y. N. Huo, J. Zhu, J. X. Li, G. S. Li, and H. X. Li, J. Catal. A **278**, 237 (2007)
[28] Z. Y. Zhao and Q. J. Liu, J. Phys. D **41**, 085417 (2008).
[29] H. T. Gao, B. Lu, X. H. Li, W. C. Liu, and G. J. Liu, J. Comput. Theor. Nanos. **10**, 1503 (2013).
[30] H. C. Wu, S. W. Lin, and J. S. Wu, J. Alloys Compd. **522**, 46 (2012).
[31] R. Asahi, T. Taga, W. Mannstadt, and A. J. Freeman, Phys. Rev. B **61**, 7459 (2000).
[32] K. S. Yang, Y. Dai, B. B. Huang, and M. H. Whangbo, J. Phys. Chem. C **113**, 2624 (2009).
[33] H. Y. Wei, Y. S. Wu, N. Lun, and F. Zhao, J. Mater. Sci. **39**, 1305 (2004).
[34] G. Kresse and J. Furthmuller, Phys. Rev. B **54**, 11169 (1996).
[35] G. Kresse and J. Furthmuller, Comput. Mater. Sci. **6**, 15 (1996).
[36] P. E. Bloöchl, Phys. Rev. B **50**, 17953 (1994).
[37] G. Kresse and D. Joubert, Phys. Rev. B **59**, 1758 (1999).
[38] J. P. Perdew, K. Burke, and M. Ernzerhof, Phys. Rev. Lett. **77**, 3865 (1996).
[39] J. P. Perdew, A. Ruzsinszky, G. I. Csonka, O. A. Vydrov, G. E. Scuseria, L. A. Constantin, X. L. Zhou, and K. Burke, Phys. Rev. Lett. **100**, 136406 (2008).
[40] H. Q. Sun, Y. Bai, H. J. Liu, W. Q. Jin, N. P. Xu, G. J. Chen, and B. Q. Xu, J. Phys. Chem. C **112**, 13304 (2008).
[41] X. C. Zhang, L. J. Zhao, C. M. Fan, Z. H. Liang, and P. D. Han, J. Phys. B **407**, 4416 (2012).
[42] S. L. Dudarev, G. A. Botton, S. Y. Savrasov, C. J. Humphreys, and A. P. Sutton, Phys. Rev. B **57**, 1505 (1998).
[43] M. E. A. Dompablo, A. M. Garcia, and M. Taravillo, J. Chem. Phys. **135**, 054503 (2011).
[44] W. G. Chen, P. F. Yuan, S. Zhang, Q. Sun, E. J. Liang, and Y. Jia, Phys. B **407**, 1038 (2012).
[45] K. K. Ghuman and C. V. Sinqh, J. Phys. **25**, 085501 (2013).
[46] Q. S. Meng, T. Wang, E. Z. Liu, X. B. Ma, Q. F. Ge, and J. L. Gong, Phys. Chem. Chem. Phys. **15**, 9549 (2013).
[47] R. Long and N. English, J. Chem. Phys. Lett. **478**, 175 (2009).
[48] A. Heller, Acc. Chem. Res. **28**, 503 (1995).
[49] R. Shirley and M. Kraft, Phys. Rev. B **81**, 075111 (2010).
[50] Z. Y. Zhao and Q. J. Liu, J. Catal. Lett. **124**, 111 (2008).
[51] J. K. Burdett, T. Hughbandks, G. J. Miller, and J. V. Smith, J. Am. Chem. Soc. **109**, 3639 (1987).
[52] K. B. Jeremy, D. P. Geoffrey, and L. P. Sarah, J. Am. Chem. Soc. **104**, 92 (1982).
[53] L. Pauling, J. Am. Chem. Soc. **51**, 1010 (1929).

DOI:10.1063/1674-0068/28/cjcp1503038